

Discrimination of neutrons and γ -rays in liquid scintillator based on

Elman neural network

**ZHANG Caixun(张才勋)¹ LIN Shinted(林兴德)² ZHAO Jianling(赵建玲)¹
WANG Li(王力)³ YU Xunzhen(余训臻)² ZHU Jingjun(朱敬军)^{1:1}
XING Haoyang(辛浩洋)^{2:2}**

*¹ Key Laboratory of Radiation Physics and Technology of Ministry of Education,
Institute of Nuclear Science and Technology, Sichuan University, Chengdu, 610065, China*

² School of Physical Science and Technology, Sichuan University, Chengdu, 610065, China

*³ Key Laboratory of Particle and Radiation Imaging (Ministry of Education) and
Department of Engineering Physics, Tsinghua University, Beijing, 100084, China*

* Supported by National Natural Science Foundation of China(11275134,11475117)

1) E-mail: zhujingjun@scu.edu.cn

2) E-mail: xhy@scu.edu.cn

Abstract

Abstract: A new neutron and γ (n/γ) discrimination method based on Elman Neural Network (ENN) was put forward to improve the n/γ discrimination performance of liquid scintillator (LS). In this study, neutron and γ data acquired from EJ-335 which was exposed in Am-Be radiation field was discriminated using ENN. The difference of n/γ discrimination performance between using ENN and Back Propagation Neural Network (BPNN) is that ENN gave a improvement over BPNN in n/γ discrimination with the increasing increasing of the Figure of Merit (FOM) from 0.907 to 0.953.

Key Words: Liquid Scintillator; n/γ discrimination; Elman neural network; BP neural network

PACS: 29.25.Dz; 29.50.+v; 07.05.Mh

1. Introduction

The technique of neutron detection is important in basic physics research, especially in the direct detection of dark matter. Since the pulse shape of nuclear recoil signals induced by WIMPs (Weakly Interactive Massive Particles), which is supposed to be the most hopeful candidate for dark matter, are the same as the pulse shape of signals induced by neutrons. Understanding the neutron background in environment is significant for dark matter research [1-4]. What's more, neutron background is always accompanied with γ radiation [5], thus, n/γ discrimination plays a key role in neutron detection. Up to now, there have been many n/γ discrimination methods, such as the Charge Compare Method (CCM) [6-7] and the Rise Time Method [8-9], which are based on analog electronic technology and complicated circuit configuration. Although these methods are good at online data analysis, they have no good performance of stability. Recently, with the development of high speed ADC, digital signal processors (DSP) and field-programmable gate arrays (FPGA), it is possible to record pulse shape of signals generated in LS completely. These new technologies prompt the study of new methods of n/γ discrimination such as fuzzy clustering analysis [10], wavelet transform [11], power spectrum gradient analysis [12] and support vector machine (SVM) [13]. As a member of non-linear science and computational intelligence science, neural network has been widely applied in pattern recognition, artificial intelligence and biological information. In 1998, Zhong et al. [14] applied the artificial neural network to n/γ discrimination at the first time. Then Esposito et al [15] and Liu et al [16] further developed the application in this field. However, the neural networks structured were all traditional BPNN, which has its own limitation in dealing with dynamic information, whereas the feedback ENN [17] has excellent property of processing

dynamic time-varying signals. So the ENN was raised to perform n/ γ discrimination combining with the randomness and time-varying characteristics of nuclear signals.

2. Pulse Shape Discrimination in Liquid Scintillator (LS)

Because of its excellent discrimination capabilities and fast time response abilities, LS is widely used for fast neutron detection. Pulse shape of light emitted by LS can usually be represented by the summation of two exponents with different time constants. The coefficients of the two exponents are determined by the ionization density of LS. The pulse shape of signal induced by neutron always has high proportion of slow component while γ is in opposite. Fig. 1 shows the average signals of neutron and γ generated in LS. The difference of pulse shape of these two kinds of signals can be used to discriminate neutron and γ signals.

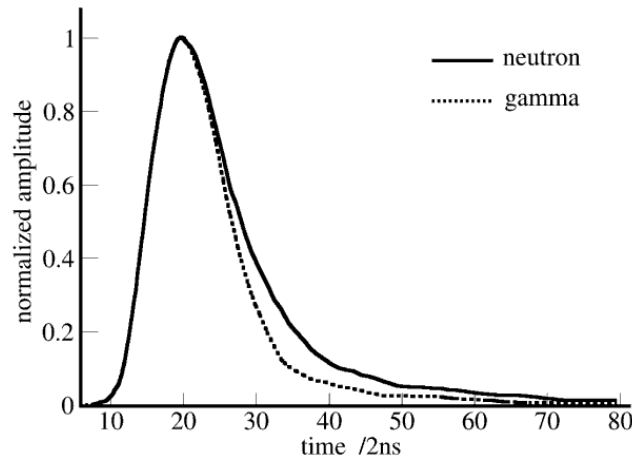


Fig. 1. The difference of pulse shape of average neutron and γ signal in EJ-335 liquid scintillator detector.

3. Elman Neural Network

The ENN is a dynamic regression neural network. It can map dynamic characteristics through storing the internal status, thus, it is able to adapt to the time-varying characteristics.

Generally the ENN is composed of 4 layers: input layer, hidden layer, output layer and a specific context layer which is an additional layer for the traditional BPNN. The input layer acts as signal transmission. The output layer plays the role of weighting linear effect. The hidden layer is a typical nonlinear activation function. The transfer function can be linear or nonlinear function. The output value of training of the hidden layer is stored in context layer through recursive connection. In the next training, the stored value is feedback to hidden layer to affect the training process which makes the network with dynamic memory. The feedback process is expressed as follows:

$$y(k)=g(w^3 \ x(k)) \quad (1)$$

$$x(k)=f(w^1 \ x_c(k)+w^2(u(k-1))) \quad (2)$$

$$x_c(k)=x(k-1) \quad (3)$$

where y is the output layer node vector, x is the hidden layer node vector, u is the input layer vector, x_c is the feedback vector, respectively. w_1 are the connection weights between the context layer and the hidden layer, w_2 are the connection weights between the input layer and the hidden layer, w_3 are the connection weights between the hidden layer and the output layer. $g(\bullet)$ is the transfer function of the output neuron and $f(\bullet)$ is the transfer function of the hidden layer neuron.

The classification performance after learning can be evaluated using the following equation:

$$E(w) = \sum_{k=1}^n [yk(w) - \bar{y}k(w)]^2 \quad (4)$$

where $yk(w)$ is the result calculated by the neural network and $\bar{y}k(w)$ is the training data set.

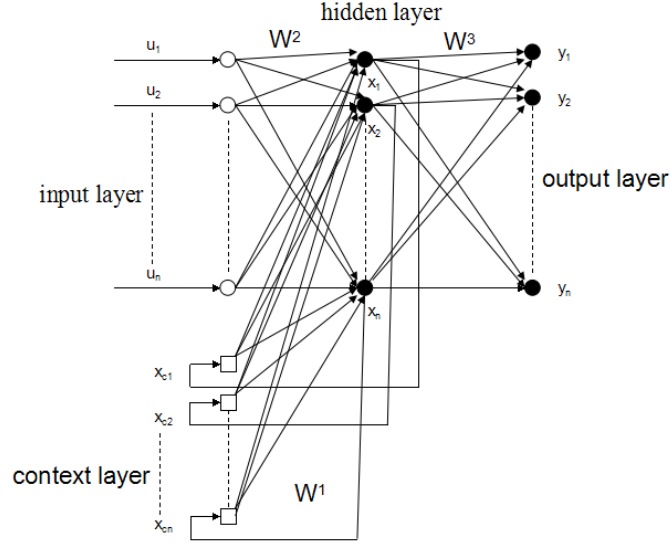


Fig. 2. Structure of Elman neural network.

4. Introduction of experiment

4.1 Experiment setup

The experimental setup is similar to that we used earlier and has been presented in detail in Yu et al. [13], here we only give a brief description. A quartz glass vessel with dimensions of 30 cm in diameter and 40 cm in length is filled with EJ-335 liquid scintillator loaded with 0.5 percent gadolinium (Gd) by weight [18]. Two 20cm HamamatsuR5912-02 photomultiplier tube (PMT) are vertically fixed at either side of the cylinder vessel. In order to enhance the light collection efficiency, Plexiglas light guides were set between the cylindrical vessel and PMTs, and interfaces of these parts are coupled by silicone grease. Signals from the anode of PMT1, PMT2 and random signal generators were separately sent to a CAEN N625 Fan-in fan-out (FIFO) plug-in which divides each signal into two circuits. One circuit signals were sent to a CAEN V1721 fast analog to digital conversion (FADC) module with 8 bit resolution working at 500M

Sample/s and the other circuit signals were sent to a CAEN N842 discriminator. And when the signals exceeds a certain threshold, the signals of PMT1 and PMT2 will pass through CAEN N405 and generate relation of logic AND. The output and the result from random trigger after discriminating will get a relation of logic OR. The result acts as a trigger signal of the V1721 FADC collected by a computer via the CAEN A2818 photoelectric conversion module and fiber. The detector is placed in a lead chamber with 5 cm thickness to shield the environment γ background. The experimental setup was shown in Fig.3.

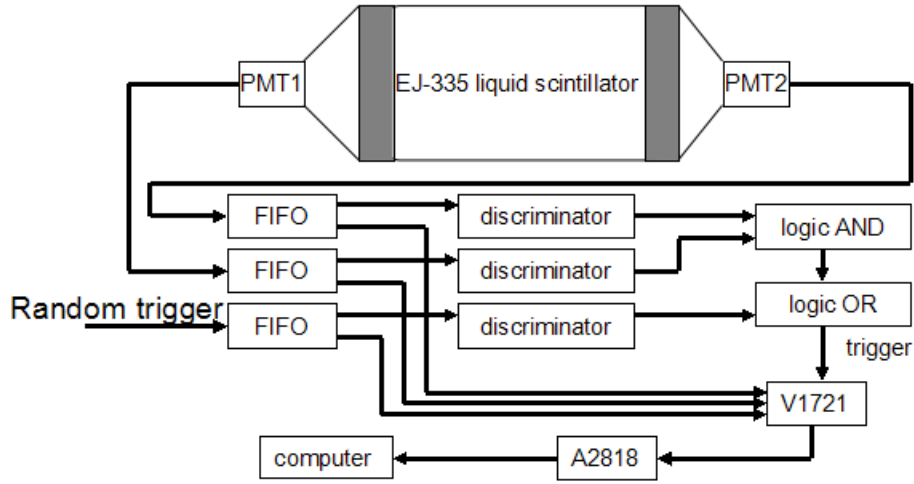


Fig. 3. Electronic and data acquisition system diagram of fast neutron detector.

3.2 Data Acquisition

In this paper, identified neutron and γ ray signals were chosen from the scatter plot by CCM to constitute the reliable training data set. As two important parameters, Q_{part} and Q_{total} were used to describe an event in CCM. These parameters are integral value of pulse amplitude corresponding to the energy deposition. Q_{total} is the corresponding integral values spanning from 20 bins before the signal peak to 80 bins after the peak. Because the difference of the pulse shape caused by neutron and γ mainly concentrated in the falling section, the tail range of a

signal was chosen as Q_{part} , and its value was obtained through the integrating from 15 bins to 80 bins after the peak. The Discrimination factor is defined as $Dis = Q_{part}/Q_{total}$. Here, the PMT1 signals were selected to perform n/γ discrimination. Due to the noise and count fluctuation, it is difficult to distinguish neutron or γ ray events in the vicinity of the gap between the two peaks with energy exceed 0.8MeV using CCM, which is plotted in Fig. 4. What's more, the pulse shape which generated by interactions between incident particles and the liquid scintillator can be described very well by a double exponential function with a correction term. The same method was used to discriminate neutron and γ ray events through fitting the pulse shapes [19]. In order to obtain the events of energy greater than 0.8 MeV, two double exponential functions were used in our paper to fit the pulse obtained from CCM.

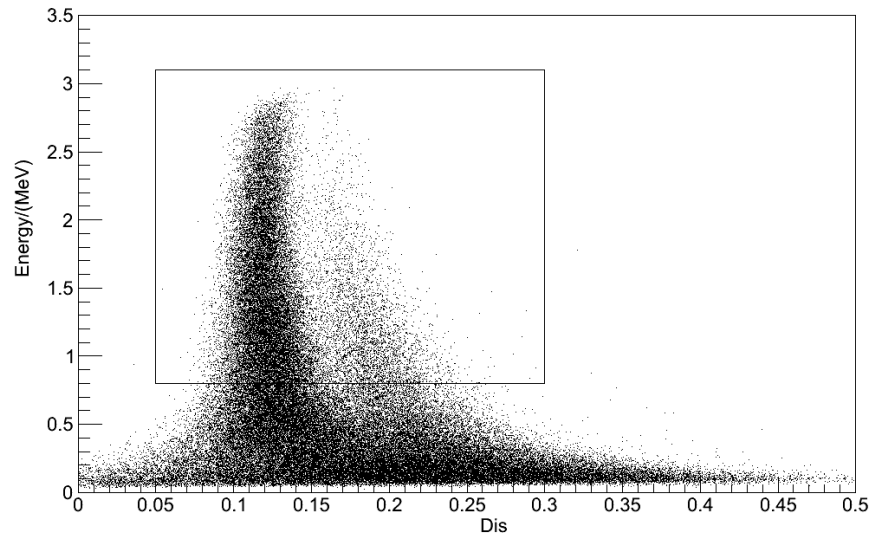


Fig. 4. The scatter plot of the Charge Compare Method(CCM).

4. Results and Discussion

The input signals of neural network normalized to eliminate the impacts which caused by the difference of the pulse amplitude. The calculation process is shown in Eq. (5):

$$x' = \frac{x - x_{\min}}{x_{\max} - x_{\min}} \quad (5)$$

where x is the pulse amplitude of a train signal, x_{\max} is the maximum pulse amplitude, x_{\min} is the minimum pulse amplitude, x' is the normalized pulse amplitude. In this study, we select 506 neutron events and 648 γ ray events as training samples of neural network. The training data set is shown in Figure. 5. Since the falling portion of neutron and γ pulse are significantly different, we selected 80 samples after peak which can sufficiently described of the falling edge of pulses to obtain a 1154×80 matrix as the neural network training data set. After many tests, the hidden layer units were selected as 20. In this experiment only neutron and γ events are to be classified, the node number of the output layer was selected as 1. The neuron transfer function Sigmoid was chosen to match the target characteristics (0-1), we think that the network output can be identified as neutron in the interval (0-0.5) and γ in the interval (0.5-1), respectively. Therefore, the Elman neural network in this study is a $80 \times 20 \times 20 \times 1$ multi-layer network.

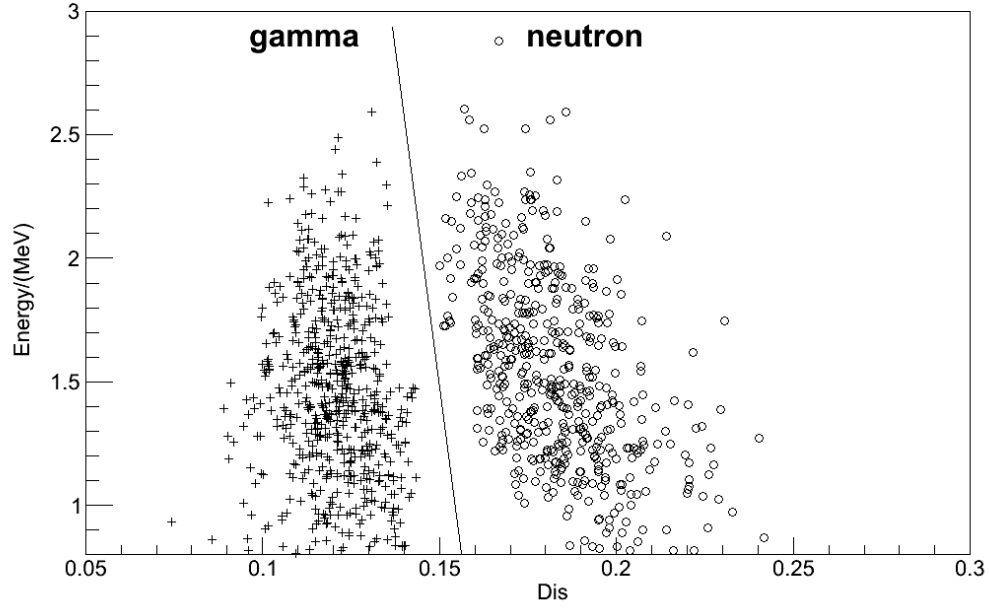


Fig. 5. The neutron and γ train data after fitted by Double exponential function.

To verify the discrimination ability of the ENN, the discrimination error ratio (DER) is defined as the ratio of the number of events incorrectly discriminated by the ENN to the total number of events of the training data set. The DER of neutron and γ is calculated with the following equations:

$$DER_{\gamma} = \frac{N_{\gamma} - N_{\gamma_ENN}}{N_{\gamma}} \times 100\% \quad (6)$$

$$DER_n = \frac{N_n - N_{n_ENN}}{N_n} \times 100\% \quad (7)$$

where N_{γ} and N_n are the testing number of γ ray and neutron, respectively. The number of γ ray and neutron events can be discriminated correctly by ENN. The result are represented by N_{γ_ENN} and N_{n_ENN} .

Table 1 Discrimination results of Elman neural network

Particle	γ	neutron
Train number	648	506
Verification number	647	504
Test number	875	644
Test result	874	642
DER_test(%)	0.11	0.30

In table 1, we can see that the ENN can effectively discriminate n/ γ events. Another way to quantitative estimate the n/ γ discrimination performance of the above two methods is the Figure of Merit (FOM) [20]. A larger value of FOM means better performance of the n/ γ discrimination and it is defined as:

$$FOM = \frac{S}{FWHM_n + FWHM_\gamma} \quad (8)$$

where S is the separation between the peaks of the neutron and γ -ray events in the spectrum, $FWHM_\gamma$ is the full-width-half-maximum (FWHM) of the spread of event classified as γ -rays and $FWHM_n$ is the FWHM of the spread in the neutron peak. If the distribution function of neutron and γ ray events in the spectrum consistent with Gaussian distribution, the FOM can be represented as Eq. 9 [21]:

$$FOM = \frac{|\mu_n - \mu_\gamma|}{2.35 \cdot (\delta_n + \delta_\gamma)} \quad (9)$$

where μ_n and μ_γ are the mean value of the neutron and γ Gaussians, respectively. δ_n and δ_γ are the standard deviation of neutron Gaussian and γ Gaussian, respectively. Fig 6 shows the ENN n/ γ discrimination result mapped by the scatter plot, in which neutron and γ events in the area above 0.8MeV can be separated clearly. And Fig 7 is the corresponding distribution

histogram to the Fig 6. The comparison between FOMs of the ENN and BPNN is reported in Table 2. Compared with the BPNN, the results indicated that ENN perform better in n/γ discrimination.

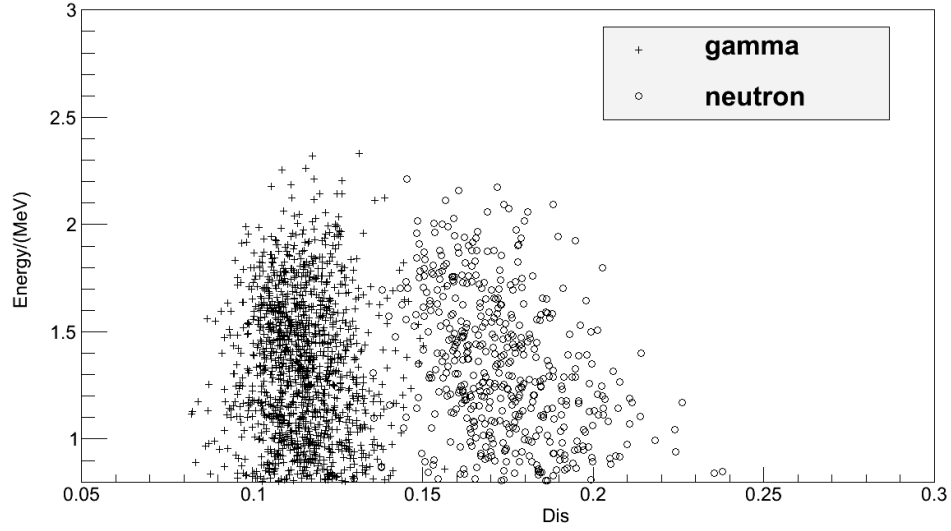


Fig. 6. The discrimination scatter plot of Elman neural network.

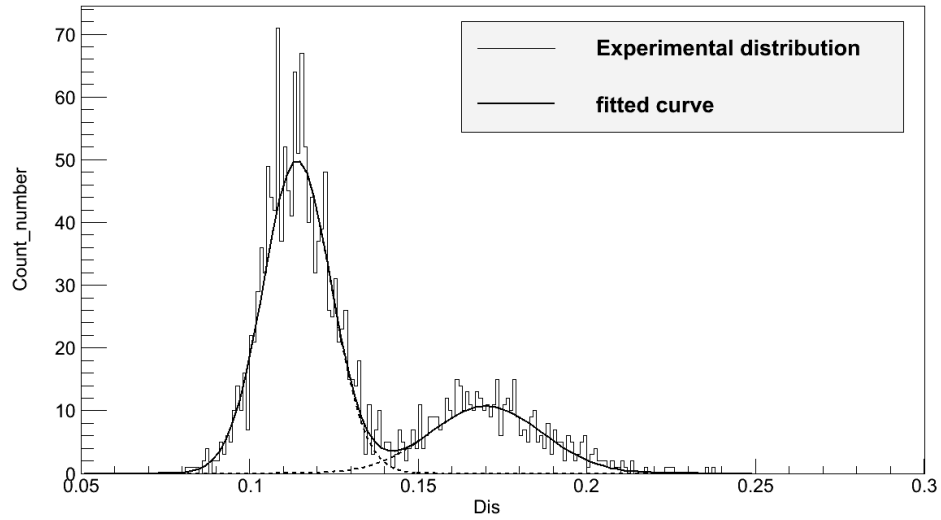


Fig. 7. The distribution histogram corresponding to Fig 6.

Table 2 Comparison between the FOM Value of Elman and BP neural network

Methods	FOM
ENN	0.953±0.0005
BPNN	0.907±0.0003

5. Results and Prospects

In this study a new method based on Elman neural network for the discrimination of neutrons and γ rays in EJ-335 liquid scintillators was presented. The training and test data set from Am-Be neutron source was acquired combination of CCM and the fitting method. The performance of the ENN in terms of n/ γ discrimination was evaluated and compared with BPNN method. The results demonstrated that ENN made the Figure of Merit (FOM) increase from 0.907 to 0.953, which means ENN has better discrimination than BPNN in n/ γ . we also believe that with the development of neural network science, this method will be more widely applied in n/ γ discrimination.

Reference:

- [1] Chaza.I.V, Brissot.R, Cavaignac.J.F et al. Astroparticle Phys, **9**(2):163-172(1989)
- [2] H. Y. Xing, L.Wang, J.J.Zhu et al. Chinese .Phys C, **37**:026003(2013)
- [3] Wulandari.H, Jochum.J, Rau.W et al. Astroparticle .Phys, **22**(3/4):313-322(2004)
- [4] Jordan.D, Tain.J.L, Algora.A et al. Astroparticle Phys, **42**:1-6(2013)
- [5] D.Z.Ding, C.Y.Ye, Z.X.Zhao et al. Neutron Physics. Beijing: Atomic Energy Press, 2001.Page 132-134(in Chinese)
- [6] Brooks.F.D. Nucl. Instrum. Methods A, **4**(2) : 151- 163(1959).
- [7] Adams.J.M, White.G. Nucl. Instrum. Methods A, **156**(3) : 459- 476(1978)
- [8] Guet.C, Signarbieus.I.C. Perrin.P et al . Nuclear Phys A, **314**(1) : 1- 4(1979)
- [9] Nowicki.L, Piasecki.E, Sobolewski.J . Nuclear Phys A, **375**(2) : 187- 192(1982)
- [10] Savran.D, Loher.B, Miklacec.M et al. Nucl. Instrum. Methods A, **624**(2):44-50(2010)
- [11] Yousefi.S, Lucchese.L, Aspinall.M.D. Nucl. Instrum. Methods A, **598**(2): 551-555(2009)
- [12] X.L.Luo,Y.K.Wang, J.Yang et.al. Nucl. Instrum. Methods A, **717**(1): 44-50(2013)
- [13] X.Z.Yu, J.J.Zhu, S.T.Lin et al. Nucl. Instrum. Methods A, **777**(1): 80-84(2015)
- [14] C.Zhong, Miller.L.F, Buckner.M. Nucl. Instrum. Methods A, **416**(2-3): 438-445(1998)
- [15] Esposito, Fortuna.L, Rizzo.A. In IEEE International joint Conference on Neural networks, **2931**-2936(2004)
- [16] Liu.G, Aspinall.M.D, Ma.X et.al. Nucl. Instrum. Methods A, **607**(3): 620-628(2009)
- [17] Elman. L.Cognitive Science, **14**(2):179-211(1990)
- [18] EJ-331 and EJ-335 Gadolinium Loaded Liquid Scintillator. <http://www.ggg-tech.co.jp/maker/eljen/ej-331.html>.
- [19] Marrone.S, Cano-Ott.D, Colonna.N et al. Nucl. Instrum. Methods A, **490**(5) : 299-307(2002)
- [20] Winyard.R.A ,Lukin.J.E ,Mcbeth.B.W. Nucl. Instrum. Methods A, **95**(1): 141-153(1971)
- [21] Liu.G ,Joyce.M.J ,Ma.X et al. IEEE.Transactions on Nuclear Science, **57**(3):1682-1691(2010)